



**Sequence stratigraphy, chemostratigraphy and facies  
analysis of Cambrian Series 2 - Series 3 boundary strata in  
northwestern Scotland**

Journal:	<i>Geological Magazine</i>
Manuscript ID	GEO-16-1505.R1
Manuscript Type:	Article
Date Submitted by the Author:	13-Aug-2016
Complete List of Authors:	Faggetter, Luke; University of Leeds, School of Earth and Environment Wignall, Paul; University of Leeds Pruss, Sara; Smith College, Department of Geosciences Sun, Yadong; University of Erlangen-Nuremburg, Geozentrum Nordbayern Raine, Robert; Geological Survey of Northern Ireland Newton, Robert; University of Leeds, School of Earth and Environment Widdowson, Mike; University of Hull, Department of Geography, Earth and Environmental Sciences (GEES) Joachimski, Michael; University of Erlangen-Nuremburg, Geozentrum Nordbayern Smith, Paul; Oxford University, Museum of Natural History
Keywords:	Durness Group, ROECE, DICE, trilobite extinction, Scotland

1  
2  
3  
4  
5  
6  
7  
8  
9  
10  
11  
12  
13  
14  
15  
16  
17  
18  
19  
20  
21  
22  
23  
24  
25  
26  
27  
28  
29  
30  
31  
32  
33  
34  
35  
36  
37  
38  
39  
40  
41  
42  
43  
44  
45  
46  
47  
48  
49  
50  
51  
52  
53  
54  
55  
56  
57  
58  
59  
60

1 **Sequence stratigraphy, chemostratigraphy and facies analysis of Cambrian**  
2 **Series 2 - Series 3 boundary strata in northwestern Scotland**

3  
4 Original article

5  
6 Luke E. Faggetter <sup>1\*</sup>, Paul B. Wignall <sup>1</sup>, Sara B. Pruss <sup>2</sup>, Yadong Sun <sup>3,7</sup>, Robert J.  
7 Raine <sup>4</sup>, Robert J. Newton <sup>1</sup>, Mike Widdowson <sup>5</sup>, Michael M. Joachimski <sup>3</sup>, M. Paul  
8 Smith <sup>6</sup>

9 <sup>1</sup> *School of Earth and Environment, University of Leeds, Woodhouse Lane, Leeds,*  
10 *LS2 9JT, United Kingdom;* <sup>2</sup> *Smith College, Department of Geosciences,*  
11 *Northampton, Massachusetts 01063, USA;* <sup>3</sup> *GeoZentrum Nordbayern, Universität*  
12 *Erlangen-Nürnberg, Schlossgarten 5, 91054 Erlangen, Germany;* <sup>4</sup> *Geological*  
13 *Survey of Northern Ireland, Dundonald House, Upper Newtownards Road,*  
14 *Ballymiscaw, Belfast, BT4 3SB, United Kingdom;* <sup>5</sup> *Department of Geography, Earth*  
15 *and Environmental Sciences (GEES), University of Hull, Hull HU6 7RX, United*  
16 *Kingdom;* <sup>6</sup> *Oxford University Museum of Natural History, Parks Road, Oxford, OX1*  
17 *3PW, United Kingdom;* <sup>7</sup> *State Key Laboratory of Geobiology and Environmental*  
18 *Geology, China University of Geosciences, Wuhan, 430074, P.R. China.*

19 Short title: Cambrian stratigraphy of northwest Scotland.

20  
21 \*Corresponding author: Luke Faggetter, email: [ee08lef@leeds.ac.uk](mailto:ee08lef@leeds.ac.uk)

22  
23 **Abstract**

24 Globally, the Series 2 – Series 3 boundary of the Cambrian coincides with a major  
25 carbon isotope excursion, sea-level changes and trilobite extinctions. Here we  
26 examine the sedimentology, sequence stratigraphy and carbon isotope record of this  
27 interval in the Cambrian strata (Durness Group) of NW Scotland. Carbonate carbon  
28 isotope data from the lower part of the Durness Group (Ghrudaidh Formation) show  
29 that the shallow-marine, Laurentian margin carbonates record two linked sea-level  
30 and carbon isotopic events. Whilst the carbon isotope excursions are not as

1  
2  
3 31 pronounced as those expressed elsewhere, correlation with global records (Sauk I/II  
4 32 boundary and *Olenellus* biostratigraphic constraint) identifies them as representing  
5 33 the local expression of ROECE and DICE. The upper part of the ROECE is recorded  
6 34 in the basal Ghrudaidh Formation whilst DICE is seen around 30 m above the base  
7 35 of this unit. Both carbon isotope excursions co-occur with surfaces interpreted to  
8 36 record regressive-transgressive events that produced amalgamated sequence  
9 37 boundaries and ravinement/flooding surfaces overlain by conglomerates of reworked  
10 38 intraclasts. The ROECE has been linked with redlichiid and olenellid trilobite  
11 39 extinctions but in NW Scotland, *Olenellus* is found after the negative peak of the  
12 40 carbon isotope excursion but before sequence boundary formation.  
13  
14  
15  
16  
17  
18  
19  
20  
21  
22  
23  
24  
25  
26  
27  
28  
29  
30  
31  
32  
33  
34  
35  
36  
37  
38  
39  
40  
41  
42  
43  
44

42 **Keywords:** Durness Group, ROECE, DICE, trilobite extinction, Scotland

## 1. Introduction

The Series 2–Series 3 transition in the Cambrian Period coincides with the first biotic crisis of the Phanerozoic, which saw major losses amongst the archaeocyathid sponges and two major trilobite groups, the redlichiids and olenellids (Palmer, 1998; Zhu *et al.* 2004; Zhu, Babcock & Peng, 2006; Guo *et al.* 2010; Fan, Deng & Zhang, 2011; Wang *et al.* 2011; Zhang *et al.* 2013; Ishikawa *et al.* 2014). Around the same time, a series of major carbon isotope oscillations have been recorded including a major negative  $\delta^{13}\text{C}$  excursion thought to coincide with the trilobite extinctions (Montañez *et al.* 2000; Zhu *et al.* 2004; Zhu, Babcock & Peng, 2006; Wang *et al.* 2011; Peng, Babcock & Cooper, 2012). The event has therefore been termed the Redlichiid-Olenellid Extinction Carbon Isotope Excursion (ROECE) (Zhu *et al.* 2004; Zhu, Babcock & Peng, 2006; Alvaro *et al.* 2008; Guo *et al.* 2010; Fan, Deng & Zhang, 2011; Wang *et al.* 2011).

The ROECE is also contemporaneous with a major regression-transgression couplet responsible for the boundary between the Sauk I and Sauk II supersequences of the Laurentian continent (Sloss, 1963; Palmer & James, 1980; Mckie, 1993; Raine & Smith, 2012). However, this sea-level change does not have an expression outside of Laurentia and, thus, has no apparent effect in Gondwana (Pratt & Bordonaro, 2014) or South China (Zhu *et al.* 2004). In contrast, its Laurentian expression is a major hiatus in shelf locations whilst down-dip a thick lowstand package is seen, such as the Hawke Bay Formation of Newfoundland – the regression has therefore been referred to as the ‘Hawke Bay event’ (Palmer & James, 1980).

The relationship between extinctions, sea-level change and C isotope excursions is a common theme in studies of environmental crises, but their interplay at this time in the Cambrian is unclear. Originally it was suggested that there were two crises: the Sinsk event (Zhuravlev & Wood, 1996), named after the widespread development of black shales in Siberia, which especially affected archaeocyathans; and a later, severe extinction of redlichiid and olenellid trilobites coinciding with the regressive Hawke Bay event (Palmer & James, 1980; Zhuravlev & Wood, 1996). However, others have also related this second crisis to the spread of anoxic waters and a negative shift of carbon isotope values (Zhu *et al.* 2004).

1  
2  
3 77 The Cambrian carbonate carbon isotope record experienced multiple  
4 78 oscillations, and correlating these excursions provides potentially the best approach  
5 79 for intercontinental correlation (e.g. Maloof *et al.* 2010; Peng, Babcock & Cooper,  
6 80 2012; Smith *et al.* 2015). At least two negative excursions occur in latest Cambrian  
7 81 Series 2, the **Archaeocyathan Extinction Carbon isotope Excursion** (AECE) (Brasier  
8 82 *et al.* 1994; Zhu, Babcock & Peng, 2006) and the ROECE. What remains unclear  
9 83 about both of these isotopic events their **relationship** to the extinction events. For  
10 84 example, while it is well established that archaeocyathans suffer a major decline at  
11 85 the Sinsk event (Zhuravlev & Wood 1996), **their** final disappearance remains  
12 86 unconstrained. In some instances, archaeocyathans are thought to extend closer to  
13 87 the Series 2/Series 3 boundary (Perejón *et al.* 2012), with a few putative occurrences  
14 88 even known from Series 3 Cambrian (Debrenne *et al.* 1984). If the archaeocyathans  
15 89 persisted to the Series 2/Series 3 boundary, the ROECE event may well be coeval  
16 90 with the last occurrence of the archaeocyathans as well as that of the redlichiid and  
17 91 olenellid trilobites.

18 92 In Series 3, the base of the Drumian Stage is defined by the first appearance  
19 93 datum (FAD) of the agnostid trilobite *Ptychagnostus atavus* which, in the Great Basin  
20 94 (USA), is associated with transgression and **the Drumian negative carbon isotope**  
21 95 **excursion (DICE)** (Babcock *et al.* 2004; 2007; Zhu *et al.* 2006; Howley and Jiang,  
22 96 2010). **The onset of the excursion commonly coincides with the FAD of *P. atavus***  
23 97 **(Montañez *et al.* 2000; Babcock *et al.* 2007) and has an amplitude of around -3 ‰ in**  
24 98 **the Great Basin and Canadian Rockies (Montañez *et al.* 2000; Howley and Jiang,**  
25 99 **2010). Elsewhere, however, the excursion is substantially less pronounced. Thus, in**  
26 100 **the carbonate record of South China (Wang *et al.* 2011) and the organic carbon**  
27 101 **record of Sweden DICE is only ~1 ‰ (Ahlberg *et al.* 2009).**

28 102 In order to further evaluate events around the Series 2–Series 3 boundary we  
29 103 have conducted a facies and sequence stratigraphical analysis of the transition  
30 104 between the An t-Sròn and Ghrudaidh formations in northwest Scotland (Fig. 1).  
31 105 Facies analysis of the Scottish strata shows a major lithological change at this level  
32 106 and recent sequence stratigraphic study has suggested that **the formational**  
33 107 **boundary** also correlates with the Sauk I/Sauk II **super**sequence boundary of North  
34 108 America (Raine & Smith, 2012). To further aid correlation, and in an attempt to  
35  
36  
37  
38  
39  
40  
41  
42  
43  
44  
45  
46  
47  
48  
49  
50  
51  
52  
53  
54  
55  
56  
57  
58  
59  
60

1  
2  
3 109 identify the  $\delta^{13}\text{C}$  changes associated with ROECE and DICE, carbonate and organic  
4 110 carbon isotope results are **presented** here.

5  
6  
7 111

## 8 9 112 **2. Geological setting and study locations**

10  
11 An almost continuous belt of Cambro-Ordovician rocks crop **out** along the  
12 Caledonian foreland within the Moine Thrust Zone of northwestern Scotland, from  
13 Loch Eriboll in the north to the Isle of Skye in the southwest (Fig. 1; **Raine & Smith,**  
14 **2012**). These strata record deposition on the southeastern Laurentian margin and  
15 are characterised by the predominance of marine sandstones of the Ardvreck Group  
16 and limestones and dolostones of the Durness Group. The Salterella Grit Member of  
17 the An t-Sròn Formation forms the uppermost part of the Ardvreck Group and  
18 consists of *Skolithos*-bioturbated cross-stratified, **quartz arenitic** sandstones (McKie,  
19 1989, 1990). The transition to the Ghrudaidh Formation of the Durness Group **marks**  
20 the establishment of a thick succession of dolostone and limestone beds that **formed**  
21 **in** a range of supratidal, peritidal and shallow marine carbonate platform deposits  
22 (Raine & Smith, 2012). Quartz sand grains persist for a few metres in the basal  
23 Ghrudaidh Formation but their disappearance at higher levels has been attributed to  
24 **an abrupt** transgression causing the sediment hinterland to become far distant  
25 (Raine & Smith, 2012).  
26  
27  
28  
29  
30  
31  
32  
33  
34  
35  
36  
37  
38

39

### 40 129 **2.a. Loch Eriboll (58°28'56.64" N, 4°40'01.01" W)**

41 130 A promontory on the western shore of Loch Eriboll is one of the few localities  
42 131 in NW Scotland in which the An t-Sròn, Ghrudaidh and the lower portion of the  
43 132 Eilean Dubh formations are well exposed without a significant tectonic break (Raine  
44 133 & Smith, 2012). The outcrop spans the upper Pipe Rock Member of the Eriboll  
45 134 Formation through the Fucoïd and Salterella Grit members, and the Ghrudaidh  
46 135 Formation to a level above its boundary with the Eilean Dubh Formation.

47  
48  
49  
50  
51 136

### 52 53 137 **2.b. Ardvreck Castle (58°10'12.51" N, 4°59'55.00" W)**

54  
55  
56  
57  
58  
59  
60

1  
2  
3 138 A road cutting along the eastern shore of Loch Assynt exposes the upper  
4 139 sections of the Salterella Grit Member, and the transition into the lowest beds of the  
5  
6 140 Ghrudaidh Formation.  
7

8 141  
9

### 10 142 **3. Methods**

11  
12  
13 143 Detailed sedimentary logging and sample collection was conducted at Loch  
14 144 Eriboll through a 52 m-thick section of siliciclastic and carbonate rocks of the  
15  
16 145 Ardvreck and Durness groups. At Ardvreck Castle, a 10 m section spanning the  
17  
18 146 same boundary was also logged. Bed numbers were allocated, and field  
19  
20 147 observations and petrographical analyses were used for lithofacies and fossil  
21 148 identification. SEM analysis (secondary and backscattered imaging and EDX  
22  
23 149 elemental mapping) was undertaken to examine more detailed petrographic features  
24  
25 150 including the nature of the pyrite content.

26  
27 151 The  $\delta^{13}\text{C}_{\text{carb}}$  and  $\delta^{18}\text{O}_{\text{carb}}$  were analysed at the GeoZentrum Nordbayern of the  
28 152 FAU Erlangen-Nürnberg, Germany. Carbonate powders were reacted with 100%  
29  
30 153 phosphoric acid at 70°C using a Gasbench II connected to a ThermoFisher Delta V  
31  
32 154 Plus mass spectrometer. All values are reported in per mil relative to V-PDB by  
33  
34 155 assigning  $\delta^{13}\text{C}$  and  $\delta^{18}\text{O}$  values of +1.95 and -2.20‰ to international standard  
35 156 NBS19 and -46.6 and -26.4‰ to international standard LSVEC, respectively.  
36  
37 157 Reproducibility monitored by replicate analyses of laboratory standards calibrated to  
38 158 NBS19 and LSVEC was  $\pm 0.07$  (1 sd) for  $\delta^{13}\text{C}$  and  $\pm 0.05$  (1 sd) for  $\delta^{18}\text{O}$ .

39  
40 159

## 41 160 **4. Facies Analysis**

### 42 161 **4.a. Loch Eriboll**

#### 43 162 *4.a.1. Salterella Grit Member*

44  
45  
46 163 The 11 m-thick Salterella Grit Member consists of beds of medium-grained,  
47 164 cross-bedded and planar and parallel laminated quartz arenites together with  
48  
49 165 strongly bioturbated quartz arenites ('pipe rock') with abundant *Skolithos* burrows  
50  
51 166 (Fig. 2). The cross-sets are stacked on low-angle bounding surfaces and in some  
52  
53 167 beds the intensity of *Skolithos* burrows is sufficient to obliterate the bedding  
54  
55 168 especially in uppermost levels where the abundance of *Salterella* also increases.  
56  
57  
58  
59  
60

1  
2  
3 169 Petrographic examination shows the original quartz grains are well sorted and range  
4 170 from well-rounded to sub-rounded (Fig. 3 G, H). Also present are thin interbeds of  
5 171 laminated mudstones and fine siltstones that display a cleavage. The contact  
6 172 between these finer beds and overlying sandstone beds commonly display small  
7 173 gutter casts.

8 174

#### 9 175 4.a.2. Ghrudaidh Formation

10 176 The Ghrudaidh Formation consists of massive, burrow-mottled and well-  
11 177 bedded dolomite beds that frequently display small vugs. The vugs have been  
12 178 interpreted to record the former presence of gypsum and anhydrite (Raine & Smith,  
13 179 2012), although they are now partly-filled with dolomite rhombs. In the absence of  
14 180 evaporitic pseudomorphs in the vugs, it is also feasible that these features are a  
15 181 remnant of volume reduction during dolomitization. Finely laminated white and dark  
16 182 grey dolomite is also present notably around 27 m above the base of the formation.  
17 183 Toward the top of the section is a ~1 m-thick (bed LE23), oolitic grainstone bed, a  
18 184 rare coarse-grained horizon. In thin section the majority of the dolomite beds consist  
19 185 of a mosaic of interlocking dolomite rhombs of silt to sand grade, which have mostly  
20 186 obliterated primary depositional fabrics. Thus, even apparently fine-grained,  
21 187 laminated dolomites seen in the field are found to be dolosparites when seen in thin  
22 188 section.

23 189 *Salterella* is the only identifiable fossil in this section of the Ghrudaidh  
24 190 Formation although other shell hash is also present (e.g. in LE9). The common  
25 191 burrows are mostly *Planolites* but there are also some branching *Thalassinoides*-like  
26 192 trace fossils.

27 193 The base of the Ghrudaidh Formation is taken at the sharp base of bed LE6  
28 194 that marks the first appearance of carbonate. It is a dark, pyritic dolomite bed  
29 195 containing carbonate nodules, which in turn is succeeded by cleaved, pyritic, vuggy  
30 196 dolomite with *Salterella* and echinoderm fragments. SEM analysis of samples from  
31 197 LE6 reveals common pyrite microcrystal agglomerations ( $\leq 10 \mu\text{m}$ ), scattered  
32 198 microcrystals and rare pyrite framboids that range in size from 5  $\mu\text{m}$  to 25  $\mu\text{m}$   
33 199 diameter. A sample from the uppermost 8 cm of LE6 also revealed the presence of  
34 200 abundant tiny halite cubes, around 10  $\mu\text{m}$  in diameter (Fig. 3, E, F; Fig. 5).

1  
2  
3 201 Bed LE7 is a microconglomerate bed that sits on a sharp, slightly erosive  
4 202 base. It grades upwards into a dolomite with common well-rounded, quartz sand  
5 203 grains. The well-rounded lithoclasts are up to 1 cm in diameter and consist of  
6 204 dolosparite. Another rudaceous horizon occurs ~25 m above the base of the  
7 205 Ghrudaidh Formation (LE17) where three thin (<10 cm-thick) erosive-based  
8 206 microconglomerates occur. The well-rounded equant pebbles are up to 1 cm in  
9 207 diameter and are composed of biomicrite (Fig. 3 B). This clast lithology is not seen in  
10 208 the underlying beds, which are recrystallized dolostones (although they appear finer-  
11 209 grained and laminated in the field).  
12  
13  
14  
15  
16  
17  
18  
19

## 20 211 **4.b. Ardvreck Castle**

### 22 212 *4.b.1. Salterella Grit Member*

23  
24  
25 213 Like the strata in the Loch Eriboll section, the upper Salterella Grit Member at  
26 214 Ardvreck Castle is dominated by quartz arenite beds with trough cross sets and  
27 215 abundant *Skolithos* burrows.  
28  
29  
30  
31

### 32 217 *4.b.2. Ghrudaidh Formation:*

33  
34  
35 218 The contact between the Salterella Grit and Ghrudaidh Formation is sharp  
36 219 and is overlain by a bed (AC3) consisting in equal amounts of well-rounded quartz  
37 220 grains and sparry dolomite that grades upward into less quartz-rich dolomite (AC4).  
38 221 This basal 1 m of the Ghrudaidh Formation is a transitional lithology that sees a  
39 222 decline in siliciclastic content and a transition to the pure dolomites that form the  
40 223 remainder of the formation. SEM examination reveals no halite crystals in these  
41 224 beds. The quartz-sand-bearing dolomite beds are sharply truncated by a thin  
42 225 microconglomerate (bed AC5) composed of small (~ 5 mm), well-rounded pebbles of  
43 226 dolomite in a matrix dominated by well-rounded quartz grains. The succeeding  
44 227 Ghrudaidh strata are dominated by beds of vuggy, burrowed, massive dolomite that  
45 228 dominate the remainder of the Formation.  
46  
47  
48  
49  
50  
51  
52

53 229

## 54 55 230 **4.c. Interpretation**

1  
2  
3 231 The Salterella Grit Member has been interpreted to be a tidal sandbank facies  
4 232 formed during a shallowing phase of deposition (McKie 1990, 1993). Conditions  
5 233 alternated between periods influenced by strong tidal currents and more quiescent  
6 234 intervals when intense burrowing occurred. The subsequent sharp transition to the  
7 235 fine-grained strata at the base of the Ghrudaidh Formation at Loch Eriboll indicates a  
8 236 considerable decrease in depositional energy. This observation, combined with the  
9 237 abundant occurrence of halite and small pyrite framboids at Loch Eriboll, suggests a  
10 238 restricted, evaporitic lagoonal setting and low oxygen conditions. The persistence of  
11 239 the well-rounded quartz grains that dominate the Salterella Grit Member, in these  
12 240 basal beds of the Ghrudaidh Formation, shows that the source terrain (probably  
13 241 aeolian dunes on the adjacent Laurentian craton) was still nearby.

14  
15  
16  
17  
18  
19  
20  
21  
22 242 The basal Ghrudaidh strata at Ardvreck Castle differs from that at Loch Eriboll  
23 243 because it has a higher proportion of quartz grains and lacks evidence (such as  
24 244 pyrite framboids and halite) for lagoonal deposition. It is possible that this is an  
25 245 intertidal facies developed immediately adjacent to aeolian dunes. However,  
26 246 contrasting facies are seen 0.9 km to the north of the Ardvreck locality at Lochan  
27 247 Feòir (NC 2367 2520), where very thinly bedded, black dolomitic mudstones  
28 248 containing abundant *Salterella* and articulated *Olenellus* aff. *reticulatus* Peach occur  
29 249 in the basal Ghrudaidh Formation (Huselbee & Thomas, 1998). The Lochan Feòir  
30 250 strata are similar to those found at Loch Eriboll suggesting that high energy and low  
31 251 energy strata show rapid lateral changes.

32  
33  
34  
35  
36  
37  
38  
39 252 The sharp truncation of the basal Ghrudaidh lagoonal/intertidal facies by a  
40 253 microconglomerate at both study locations is interpreted to record the passage of a  
41 254 zone of erosion (see sequence stratigraphic discussion below) and heralded the  
42 255 establishment of persistently well-oxygenated conditions, as shown by the  
43 256 bioturbation and shelly fossils in the overlying fine-grained dolostones (now mostly  
44 257 recrystallized). The gradual loss of rounded quartz grains upsection indicates an  
45 258 increasingly more distant source terrain (Raine & Smith, 2012). The low-energy  
46 259 conditions were occasionally punctuated by much higher energy conditions recorded  
47 260 by the rare oolitic strata. The frequent vuggy appearance of the strata suggests  
48 261 replacement of secondary evaporites as a result of concentrated pore-fluid brines.  
49 262 The elevated salinity is interpreted to have occurred late in deposition of the  
50 263 Ghrudaidh Formation.  
51  
52  
53  
54  
55  
56  
57  
58  
59  
60

1  
2  
3 264 The bedset LE16-18 records a shift in conditions as the intensely burrowed  
4 265 strata is replaced by laminated dolomites and then a thin, erosive-based  
5 266 microconglomerate. This succession is similar to the strata that are seen at the base  
6 267 of the Ghrudaidh Formation where lagoonal beds were truncated during  
7 268 transgression.  
8  
9  
10

11 269

## 12 270 5. Chemostratigraphy

13  
14  
15  
16 271 This study presents the first  $\delta^{13}\text{C}$  and  $\delta^{18}\text{O}$  chemostratigraphic data for the  
17 272 Durness Group. A total of 20 samples from Ardvreck Castle were analysed, of which  
18 273 two samples from the Salterella Grit had insufficient carbonate content to yield a  
19 274 signal. In addition 40 samples from Loch Eriboll were analysed, and three were  
20 275 found to be too carbonate poor to yield a reliable value.  
21  
22  
23

24  
25 276 At Loch Eriboll, the lowest  $\delta^{13}\text{C}_{\text{carb}}$  value is returned from the Salterella Grit  
26 277 Member, sample AS46 with a TIC of 4.5 wt % returned from Salterella shells.  
27 278 Although this is found in a sandstone we interpret the organic source of the  
28 279 carbonate to represent an original environmental signal. Above this  $\delta^{13}\text{C}_{\text{carb}}$  values of  
29 280 -3.0 ‰ occur in the silty dolomites immediately above at the base of the Ghrudaidh  
30 281 Formation (Fig. 5). These were followed by an increase in the overlying 10 m  
31 282 culminating in peak positive values of -0.4 ‰ before a decline to a broad lowpoint of  
32 283 -2 ‰ around 30 m above the base of the formation. The curve then swings to  
33 284 heavier values of -0.6‰ and then falls to -1.6‰ at the top of the Loch Eriboll section.  
34 285 The shorter Ardvreck Castle  $\delta^{13}\text{C}_{\text{carb}}$  record (Fig. 5) shows a rapid increase across  
35 286 the Salterella Grit/Ghrudaidh boundary to a positive peak 2 m above before  
36 287 declining. The two lowest values measured from the Salterella Grit Member at the  
37 288 base of the section come from sandstones in which the main carbonate content is  
38 289 the shells of *Salterella* (carbonate content ranges from 1 to 7 wt %, see data table).  
39 290 The positive hump of  $\delta^{13}\text{C}_{\text{carb}}$  values seen at both location and is considered to  
40 291 record the same chemostratigraphic event. However, at Ardvreck Castle this  
41 292 excursion occurs over a shorter interval (Fig. 5), an observation we attribute to a  
42 293 more condensed section at this location.  
43  
44  
45  
46  
47  
48  
49  
50  
51  
52  
53  
54

55 294 The  $\delta^{18}\text{O}_{\text{carb}}$  values at both the Loch Eriboll and Ardvreck Castle locations  
56 295 show slight covariance with  $\delta^{13}\text{C}_{\text{carb}}$  values only in samples taken from the Salterella  
57  
58  
59  
60

1  
2  
3 296 Grit Member (Fig. 5 inset). The two lightest  $\delta^{18}\text{O}_{\text{carb}}$  values that also correspond with  
4 297 the lightest  $\delta^{13}\text{C}_{\text{carb}}$  values (Fig. 3) are from the sandstones of the Salterella Grit at  
5 298 Ardvreck Castle (see data table). In this member the main source of carbonate are  
6 299 the shells of *Salterella* and the carbonate content is significant enough (1-8 wt% TIC)  
7 300 to measure a carbonate carbon isotope signal. Whilst it is possible that this slight  
8 301 covariation is a reflection of an early diagenetic signal, at Loch Eriboll the strong  
9 302 similarity between Salterella Grit  $\delta^{13}\text{C}_{\text{carb}}$  values (-2.98‰) and basal Ghrudaidh  
10 303 Formation values (-2.84‰) suggests that the Salterella Grit lowest data point at Loch  
11 304 Eriboll is in accordance with a reliable primary isotopic signal from the Ghrudiadh  
12 305 Formation. This observation suggests that  $\delta^{13}\text{C}_{\text{carb}}$  values have not been affected by  
13 306 significant diagenesis and that the returning limb of ROECE recorded within the  
14 307 Salterella Grit and immediately above in the Ghrudaidh Formation is a primary  
15 308 record of oceanic carbon isotope fluctuations.

16 309 The  $\delta^{13}\text{C}_{\text{org}}$  record we obtained (Table 1) shows frequent oscillations with no  
17 310 consistent trends between the sections nor any similarity with the  $\delta^{13}\text{C}_{\text{carb}}$  curve. This  
18 311 variability probably relates to the extremely low total organic carbon values (mostly <  
19 312 0.5 %) and the likelihood that values are influenced by factors such as reworked,  
20 313 detrital organic carbon.

#### 21 314 Interpretation

22 315 Global oscillations in the Cambrian  $\delta^{13}\text{C}_{\text{carb}}$  record include the ROECE, a  
23 316 major negative excursion developed around the Series 2/3 boundary during which  
24 317 values drop to -4‰ followed by a rapid recovery to heavier values (Montañez *et al.*  
25 318 2000; Guo *et al.* 2010). From the Scottish data, we interpret the abrupt rise of  
26 319  $\delta^{13}\text{C}_{\text{carb}}$  at the base of the Ghrudaidh Formation to record this recovery phase. The  
27 320 amplitude of ROECE varies considerably between regions. Laurentian values are  
28 321 around 4.5‰, in China it can reach 7‰ but in Siberia it is only 1.5‰ (Wang *et al.*  
29 322 2011). In Scotland the excursion is 3‰ but this is likely not the full amplitude  
30 323 because the lowpoint of the curve is not recorded in the carbonate-free clastic  
31 324 sediments of the lower Salterella Grit.

32 325 The oscillations of  $\delta^{13}\text{C}_{\text{carb}}$  values within the higher levels of the Ghrudaidh  
33 326 Formation (only studied at Loch Eriboll) can be closely matched with the global curve  
34 327 (Fig. 3) and they suggest that the prolonged lowpoint of values ~30 m above the

1  
2  
3 328 base of the Ghrudaidh Formation (beds LE 16-18) could be DICE, an excursion that  
4 329 marks the Stage 5-Drumian stage age. As with ROECE, DICE varies considerably in  
5 330 magnitude. In South China it ranges from 1.0 to 2.5 ‰ but in the Great Basin of the  
6 331 western United States it is present as a 3.5 ‰ negative excursion (Zhu *et al.* 2004;  
7 332 Howley & Jiang 2010). The larger values in the USA may reflect the exacerbation of  
8 333 the excursion by regional factors such as upwelling of deep oceanic waters and/or  
9 334 erosion from newly uplifted mountains (Howley and Jiang 2010). The amplitude of  
10 335 DICE in Scotland is towards the lower end of this reported range, with a magnitude  
11 336 of ~1 ‰.

12  
13  
14  
15  
16  
17  
18 337 Our chemostratigraphic age assignment for the Ghrudaidh Formation is also  
19 338 supported by the modest biostratigraphic data that is available. The single *Olenellus*  
20 339 reported from basal beds of the Ghrudaidh Formation (Huselbee & Thomas 1998),  
21 340 indicates a late Series 2 age. The presence of *Salterella* up to 10 m above the base  
22 341 of the formation also indicates a Series 2 age (Fritz & Yochelson, 1988; Wright &  
23 342 Knight, 1995). No other biostratigraphically useful fossils occur but Wright & Knight  
24 343 (1995) argued that the higher levels of the Ghrudaidh Formation correlated with the  
25 344 Bridge Cove Member of the March Point Formation in western Newfoundland. This  
26 345 age assignment places the Scottish strata above the 10 m level in our logs within the  
27 346 early part of Series 3. This is in agreement with our recognition of DICE 30 m above  
28 347 the base of the Ghrudaidh Formation at Loch Eriboll.

## 37 348 **6. Sequence stratigraphy**

38  
39 349 The sequence stratigraphy of the Cambro-Ordovician succession of northwest  
40 350 Scotland was discussed by Raine & Smith (2012) who placed the boundary between  
41 351 Sloss's (1963) Sauk I and Sauk II supersequences at the An t-Sròn/Ghrudaidh  
42 352 formational boundary. In North America, this supersequence boundary is a major  
43 353 hiatal surface that formed during the Hawke Bay Event (Wright & Knight, 1995), but it  
44 354 is not clearly manifested outside of Laurentia (e.g. Alvaro & Debrenne, 2010; Pratt &  
45 355 Bordonaro, 2014). Northwest Scotland lay on the Laurentian margin and so this  
46 356 shallow-water setting might be expected to show a well-developed sequence  
47 357 boundary. However, the effect of the Hawke Bay event was surprisingly subdued.  
48 358 The formational boundary marks the culmination of prolonged shallowing and sees  
49 359 the transition from open, inner shelf conditions of the uppermost *Salterella* Grit to the  
50 360 restricted, lagoonal and intertidal facies of the basal Ghrudaidh Formation. This base

1  
2  
3 361 level shift, from inner shelf to lagoon, is probably no more than 10 m. A few metres  
4 362 higher a ravinement surface marks the onset of flooding and modest deepening:  
5 363 again base-level changes are only of the order of a few metres. There are two  
6 364 options for the placement of a sequence boundary in this succession. The first would  
7 365 place it at the formational contact. **This would imply that** the overlying  
8 366 lagoonal/intertidal facies are a thin development of a lowstand systems tract with its  
9 367 top boundary being an initial flooding (ravinement) surface. The second option would  
10 368 consider the ravinement surface **to be amalgamated with a** sequence boundary and  
11 369 with the formational boundary only recording a facies change. Given the overall inner  
12 370 platform setting of the Scottish outcrops it is perhaps unlikely that any lowstand  
13 371 strata would be developed, because such sediment packages are typically found  
14 372 distally in offshore/shelf margin locations. Therefore **we consider the second option**  
15 373 **to be the most probable. Thus the sequence boundary is developed low in the**  
16 374 **Ghrudaidh Formation and not at its base. It is likely to** record a major hiatus. The  
17 375 halite crystals developed immediately below the surface at Loch Eriboll may have  
18 376 grown during this non-depositional episode in a supratidal setting. The succeeding  
19 377 20 m-thick succession of dolomicrites do not record major facies changes but the  
20 378 **significant** up-section decline of terrigenous material **suggests** continued  
21 379 transgression and flooding of the hinterland.

22  
23  
24  
25  
26  
27  
28  
29  
30  
31  
32  
33  
34  
35 380 The next major facies change is centred on another thin microconglomerate  
36 381 (bed LE17). It is similar to the lower examples, and is also interpreted to have formed  
37 382 during ravinement. By comparison with the basal Ghrudaidh Formation, the finely  
38 383 laminated strata that underlie this bed (LE16) may be highstand lagoonal facies.  
39 384 Thus, this succession of Beds (LE16 - 18), **chemostratigraphically correlated with** the  
40 385 Stage 5-Drumian boundary, probably records the regressive-transgressive couplet  
41 386 seen elsewhere in the world at this level (e.g. Montañez *et al.* 1996; Babcock *et al.*  
42 387 2004; Alvaro *et al.* 2013).

43  
44  
45  
46  
47  
48  
49 388

## 50 51 389 **7. Conclusions**

52  
53 390 The NW Scotland sections reveal a clear sequence of events across the Series 2–  
54 391 Series 3 boundary and help evaluate some of the cause-and-effect relationships of  
55 392 this **dynamic interval**.

1  
2  
3 393 The later part of the ROECE is preserved in the  $\delta^{13}\text{C}_{\text{carb}}$  record of the basal  
4 394 Ghrudaidh Formation with the lowpoint of this excursion probably occurring earlier  
5 395 during deposition of the Salterella Grit Member. Sequence boundary formation  
6 396 (perhaps the equivalent of the Hawke Bay event in North America) lead to the  
7 397 development of an **erosive surface by ravinement processes that is mantled by a thin**  
8 398 **conglomerate** near the base of the Ghrudaidh Formation. The overlying strata  
9 399 records transgression with an increasingly distal hinterland supplying. No lowstand  
10 400 facies are developed because of the proximal setting on this Laurentian platform.  
11 401 **The formational boundary, 2 m below the sequence boundary, is interpreted to be**  
12 402 **simply a facies contact that marks coastal progradation with inner shelf tidal clastic**  
13 403 **facies replaced by intertidal clastics and dolomitic lagoonal facies.**

14 404 The Stage 5/Drumian boundary, identified from carbon isotope oscillations  
15 405 (DICE), is found within the upper Ghrudaidh Formation and this too records an  
16 406 amalgamated sequence boundary/flooding surface with lagoonal facies transgressed  
17 407 by a conglomerate developed on a ravinement surface. The base of the Drumian in  
18 408 Gondwana is marked by the spread of anoxic facies by marine transgression (Alvaro  
19 409 *et al.* 2013). This level is also associated with trilobite turnover but the lack of fossils  
20 410 in the Scottish strata does not permit evaluation of this event. However, elsewhere in  
21 411 the world the earliest Drumian saw a major transgression and spread of anoxic  
22 412 facies, especially in Gondwanan sections (Alvaro *et al.* 2013). From our section at  
23 413 Loch Eriboll the dark grey, laminated dolomites (LE 18) could be a Laurentian  
24 414 development of this transgressive anoxic phase.

25 415 *Olenellus* occurs in the basal Ghrudaidh Formation within the highstand  
26 416 facies, but below the sequence boundary. Thus, the ROECE extinctions, which  
27 417 removed the olenellids, may have post-dated the peak negative values of ROECE. A  
28 418 similar post-excursion extinction of redlichiid trilobites is also seen in South China  
29 419 (Montañez *et al.* 2000; Zhu *et al.* 2004; Peng, Babcock & Cooper, 2012). **This has a**  
30 420 **bearing on proposed extinction mechanisms.** Montañez *et al.* (2000) argued that the  
31 421 incursion of deep anoxic waters (with a light carbon isotope signature derived from  
32 422 remineralized organic matter), into shallower waters may have triggered a biomass  
33 423 crash and trilobite extinction. The mistiming of the ROECE and extinctions in  
34 424 Scotland (and also in China eg. Zhu *et al.* 2004) does not support this scenario.  
35 425 However, trilobites are exceptionally rare in the Ghrudaidh Formation and it is

1  
2  
3 426 possible that the occasional *Olenellus* fossils are holdovers that post-date the main  
4 427 extinction. Further collecting is required in more fossiliferous sections worldwide to  
5  
6 428 fully evaluate this extinction event.  
7

8  
9 429

10 430 **Acknowledgements.** This research was made possible by a NERC postgraduate  
11 431 studentship and a postgraduate Student Bursary grant (March 2014) from the  
12 432 Mineralogical Society of Great Britain and Ireland and the use of the Stable Isotope  
13 433 Laboratory at Friedrich-Alexander University, Erlangen-Nürnberg. We thank two  
14 434 anonymous reviewers for their feedback.  
15  
16  
17  
18  
19

20 435

21 436 Figure captions:

22  
23  
24 437 Figure 1. Locality map of the study locations (LE- Loch Eriboll, AC- Ardvreck Castle)  
25 438 in northwest Scotland, modified from Raine and Smith (2012), and summary of  
26 439 Lower-Middle Cambrian stratigraphic units in the region.  
27  
28

29 440 Figure 2. Sedimentary logs of the Loch Eriboll and Ardvreck Castle sections showing  
30 441 the correlation of a ravinement surface near the base of the Ghrudaidh Formation.  
31 442 and a second surface ~27m above the base of the Formation at Loch Eriboll.  
32  
33

34 443 Figure 3. Photomicrographs of Ghrudaidh Formation facies. A: dolosparite pebble  
35 444 (highlighted with dotted line) in a sandy dolomicrite matrix, LE 17. B: Scan of slide of  
36 445 rudaceous limestone, exhibiting well-rounded, micrite clasts in a dolosparite matrix.  
37 446 C: Rudaceous limestone of bed LE17 showing irregularly shaped, sparry bioclasts in  
38 447 an intraclast. D: Photomicrograph of sandy/silty dolomite from the base of the  
39 448 Ghrudaidh Formation at Ardvreck Castle consisting of equal portions of rounded  
40 449 (aeolian) quartz grains and dolomite microspar (AC 3). E, F: Backscatter SEM  
41 450 images of LE 6 lagoonal facies. Bright white cubes are halite, mid grey is a fine  
42 451 dolomite matrix and the largest, dull grey grains in E are aeolian quartz silt and fine  
43 452 sand. G: Photomicrographs from Ardvreck Section. *Salterella* shell amongst well  
44 453 rounded quartz grains of the Salterella Grit, (Bed AC 1). H: Rounded silt and fine  
45 454 sand grains, a relatively poorly sorted lithology from Bed AC 1.  
46  
47  
48  
49  
50  
51  
52  
53  
54

55 455 Figure 4. Representative EDS spectra taken from a halite cube in bed LE 6.  
56  
57  
58  
59  
60

1  
2  
3 456 Figure 5.  $\delta^{13}\text{C}_{\text{carb}}$  chemostratigraphic curve from Loch Eriboll and Arvreck sections.  
4 457 Top right inset is a cross-plot of C and O data with samples from the Salterella Grit  
5 458 Member and Ghrudaidh Fm from each location delineated by respective symbols.  
6 459 The reported occurrence of *Olenellus* is from Huselbee & Thomas, 1998, the precise  
7 460 location of the specimen is unknown but is indicated by dashed line.  
8 461 Figure 6. Global Cambrian carbon isotope curve (Zhu *et al.* 2006) showing the  
9 462 proposed correlation with the Scottish sections.  
10  
11  
12  
13  
14  
15  
16  
17  
18  
19  
20  
21  
22  
23  
24  
25  
26  
27  
28  
29  
30  
31  
32  
33  
34  
35  
36  
37  
38  
39  
40  
41  
42  
43  
44  
45  
46  
47  
48  
49  
50  
51  
52  
53  
54  
55  
56  
57  
58  
59  
60

Proof For Review

463 **References:**

- 464 AHLBERG, P. E. R., AXHEIMER, N., BABCOCK, L. E., ERIKSSON, M. E., SCHMITZ, B., &  
465 TERFELT, F. 2009. Cambrian high-resolution biostratigraphy and carbon isotope  
466 chemostratigraphy in Scania, Sweden: first record of the SPICE and DICE  
467 excursions in Scandinavia. *Lethaia*, **42(1)**, 2-16.
- 468 ÁLVARO, J. J., BAULUZ, B., SUBÍAS, I., PIERRE, C., & VIZCAÍNO, D. 2008. Carbon  
469 chemostratigraphy of the Cambrian-Ordovician transition in a midlatitude mixed  
470 platform, Montagne Noire, France. *Geological Society of America Bulletin*,  
471 **120(7-8)**, 962-975.
- 472 **ÁLVARO, J. J., & DEBRENNE, F. 2010. The Great Atlasian Reef complex: an early**  
473 **Cambrian subtropical fringing belt that bordered West**  
474 **Gondwana. *Palaeogeography, Palaeoclimatology, Palaeoecology*, **294(3)**, 120-  
475 **132.****
- 476 ÁLVARO, J. J., AHLBERG, P., BABCOCK, L. E., BORDONARO, O. L., CHOI, D. K., COOPER,  
477 R. A., & JAGO, J. B. 2013. Global Cambrian trilobite palaeobiogeography  
478 assessed using parsimony analysis of endemism. *Geological Society, London*,  
479 *Memoirs*, **38(1)**, 273-296.
- 480 BABCOCK, L. E., REES, M. N., ROBISON, R. A., LANGENBURG, E. S., & PENG, S. 2004.  
481 Potential Global Standard Stratotype-section and Point (GSSP) for a Cambrian  
482 stage boundary defined by the first appearance of the trilobite *Ptychagnostus*  
483 *atavus*, Drum Mountains, Utah, USA. *Geobios*, **37(2)**, 149-158.
- 484 BABCOCK, L. E., ROBISON, R. A., REES, M. N., PENG, S., & SALTZMAN, M. R. 2007. The  
485 global boundary stratotype section and point (GSSP) of the Drumian Stage  
486 (Cambrian) in the Drum Mountains, Utah, USA. *Episodes*, **30(2)**, 85.
- 487 BRASIER, M. D., CORFIELD, R. M., DERRY, L. A., ROZANOV, A. Y., & ZHURAVLEV, A. Y.  
488 1994. Multiple  $\delta^{13}\text{C}$  excursions spanning the Cambrian explosion to the  
489 Botomian crisis in Siberia. *Geology*, **22(5)**, 455-458.
- 490 BRASIER, M. D., & SUKHOV, S. S. 1998. The falling amplitude of carbon isotopic  
491 oscillations through the Lower to Middle Cambrian: northern Siberia  
492 data. *Canadian Journal of Earth Sciences*, **35(4)**, 353-373.
- 493 DEBRENNE, F., ROZANOV, A. Y., & WEBERS, G. F. 1984. Upper Cambrian

- 1  
2  
3 494 Archaeocyatha from Antarctica. *Geological Magazine*, **121(04)**, 291-299.
- 4  
5 495 FAN, R., DENG, S., & ZHANG, X. 2011. Significant carbon isotope excursions in the  
6 496 Cambrian and their implications for global correlations. *Science China Earth  
7 497 Sciences*, **54(11)**, 1686-1695.
- 8  
9 498 FRITZ, W. H., & YOCHELSON, E. L. 1988. The status of *Salterella* as a Lower Cambrian  
10 499 index fossil. *Canadian Journal of Earth Sciences*, **25(3)**, 403-416.
- 11  
12 500 GOZALO, R., ÁLVAREZ, M. E. D., VINTANED, J. A. G., ZHURAVLEV, A. Y., BAULUZ, B.,  
13 501 SUBÍAS, I., MARTORELL, J.B.C., MAYORAL, E., GURSKY, H., ANDRÈS, J.A. & LIÑÁN,  
14 502 E. 2013. Proposal of a reference section and point for the Cambrian Series 2–3  
15 503 boundary in the Mediterranean subprovince in Murero (NE Spain) and its  
16 504 intercontinental correlation. *Geological Journal*, **48(2-3)**, 142-155.
- 17  
18 505 GUO, Q., STRAUSS, H., LIU, C., ZHAO, Y., YANG, X., PENG, J., & YANG, H. 2010. A  
19 506 negative carbon isotope excursion defines the boundary from Cambrian Series  
20 507 2 to Cambrian Series 3 on the Yangtze Platform, South China.  
21 508 *Palaeogeography, Palaeoclimatology, Palaeoecology*, **285(3)**, 143-151.
- 22  
23 509 HOWLEY, R. A., & JIANG, G. 2010. The Cambrian Drumian carbon isotope excursion  
24 510 (DICE) in the Great Basin, western United States. *Palaeogeography,  
25 511 Palaeoclimatology, Palaeoecology*, **296(1)**, 138-150.
- 26  
27 512 HUSELBEE, M. Y., & THOMAS, A. T. 1998. *Olenellus* and conodonts from the Durness  
28 513 Group, NW Scotland, and the correlation of the Durness succession. *Scottish  
29 514 Journal of Geology*, **34(1)**, 83-88.
- 30  
31 515 ISHIKAWA, T., UENO, Y., SHU, D., LI, Y., HAN, J., GUO, J. & KOMIYA, T 2014. The  $\delta^{13}\text{C}$   
32 516 excursions spanning the Cambrian explosion to the Canglangpuian mass  
33 517 extinction in the Three Gorges area, South China. *Gondwana Research*, **25(3)**,  
34 518 1045-1056.
- 35  
36 519 MALOOF, A. C., PORTER, S. M., MOORE, J. L., DUDÁS, F. Ö., BOWRING, S. A., HIGGINS, J.  
37 520 A., ... & EDDY, M. P. 2010. The earliest Cambrian record of animals and ocean  
38 521 geochemical change. *Geological Society of America Bulletin*, **122(11-12)**, 1731-  
39 522 1774.
- 40  
41  
42  
43  
44  
45  
46  
47  
48  
49  
50  
51  
52  
53  
54  
55  
56  
57  
58  
59  
60

- 1  
2  
3 523 MCKIE, T. 1989. Barrier island to tidal shelf transition in the early Cambrian Eriboll  
4 524 Sandstone. *Scottish Journal of Geology*, **25(3)**, 273-293.
- 5  
6 525 MCKIE, T. 1990. Tidal and storm influenced sedimentation from a Cambrian  
7 526 transgressive passive margin sequence. *Journal of the Geological*  
8 527 *Society*, **147(5)**, 785-794.
- 9  
10  
11  
12 528 MCKIE, T. 1993. Relative sea-level changes and the development of a Cambrian  
13 529 transgression. *Geological Magazine*, **130(02)**, 245-256.
- 14  
15  
16 530 MONTAÑEZ, I. P., BANNER, J. L., OSLEGER, D. A., BORG, L. E., & BOSSERMAN, P. J. 1996.  
17 531 Integrated Sr isotope variations and sea-level history of Middle to Upper  
18 532 Cambrian platform carbonates: Implications for the evolution of Cambrian  
19 533 seawater  $^{87}\text{Sr}/^{86}\text{Sr}$ . *Geology*, **24(10)**, 917-920.
- 20  
21  
22  
23 534 MONTAÑEZ, I. P., OSLEGER, D. A., BANNER, J. L., MACK, L. E., & MUSGROVE, M. 2000.  
24 535 Evolution of the Sr and C isotope composition of Cambrian oceans. *GSA*  
25 536 *today*, **10(5)**, 1-7.
- 26  
27  
28 537 PALMER, A. R. 1998. Terminal early Cambrian extinction of the Olenellina:  
29 538 documentation from the Pioche Formation, Nevada. *Journal of Paleontology*,  
30 539 **72(04)**, 650-672.
- 31  
32  
33  
34 540 PALMER, A. R., & JAMES, N. P. 1980. The Hawke Bay event: a circum-lapetus  
35 541 regression near the Lower–Middle Cambrian boundary. *The Caledonides in the*  
36 542 *USA*, **2**, 15-18.
- 37  
38  
39  
40 543 PENG, S., BABCOCK, L. E., & COOPER, R. A. 2012. The Cambrian Period. In *The*  
41 544 *Geologic Time Scale (2012) 2-Volume Set*. (eds Gradstein, F.M.; Ogg, G.&  
42 545 Schmitz, M.), pp.437-488, Elsevier.
- 43  
44  
45 546 PEREJÓN, A., MORENO-EIRIS, E., BECHSTÄDT, T., MENÉNDEZ, S., & RODRÍGUEZ-  
46 547 MARTÍNEZ, M. 2012. New Bilbilian (early Cambrian) archaeocyath-rich  
47 548 thrombolitic microbialite from the Láncara Formation (Cantabrian Mts., northern  
48 549 Spain). *Journal of Iberian Geology*, **38(2)**, 313-330.
- 49  
50  
51 550 PRATT, B. R., & BORDONARO, O. L. 2014. Early middle Cambrian trilobites from La  
52 551 Laja Formation, Cerro El Molle, Precordillera of western Argentina. *Journal of*  
53 552 *Paleontology*, **88(5)**, 906-924.
- 54  
55  
56  
57  
58  
59  
60

- 1  
2  
3 553 RAINE, ROBERT J., & M. PAUL SMITH, 2012. Sequence stratigraphy of the Scottish  
4 554 Laurentian margin and recognition of the Sauk megasequence, in *The great*  
5 555 *American carbonate bank: The geology and economic resources of the*  
6 556 *Cambrian– Ordovician Sauk megasequence of Laurentia* (eds J. R. Derby, R.  
7 557 D. Fritz, S. A. Longacre, W. A. Morgan, and C. A. Sternbach), pp 575-598  
8 558 AAPG Memoir 98.
- 9  
10  
11  
12  
13 559 SLOSS, L. L. 1963. Sequences in the cratonic interior of North America. *Geological*  
14 560 *Society of America Bulletin*, **74(2)**, 93-114.
- 15  
16  
17 561 SMITH, E. F., MACDONALD, F. A., PETACH, T. A., BOLD, U., & SCHRAG, D. P. 2015.  
18 562 Integrated stratigraphic, geochemical, and paleontological late Ediacaran to  
19 563 early Cambrian records from southwestern Mongolia. *Geological Society of*  
20 564 *America Bulletin*, **128(3-4)**, 442-468.
- 21  
22  
23  
24 565 WANG, X., HU, W., YAO, S., CHEN, Q., & XIE, X. 2011. Carbon and strontium isotopes  
25 566 and global correlation of Cambrian Series 2-Series 3 carbonate rocks in the  
26 567 Keping area of the northwestern Tarim Basin, NW China. *Marine and*  
27 568 *Petroleum Geology*, **28(5)**, 992-1002.
- 28  
29  
30  
31 569 WRIGHT, D. T., & KNIGHT, I. 1995. A revised chronostratigraphy for the lower Durness  
32 570 Group. *Scottish Journal of Geology*, **31(1)**, 11-22.
- 33  
34  
35 571 ZHANG, W., SHI, X., JIANG, G., TANG, D., & WANG, X. 2013. Mass-occurrence of  
36 572 oncoids at the Cambrian Series 2–Series 3 transition: Implications for microbial  
37 573 resurgence following an Early Cambrian extinction. *Gondwana Research*.  
38 574 **28(1)**, 432-450.
- 39  
40  
41  
42 575 ZHU, M. Y., ZHANG, J. M., LI, G. X., & YANG, A. H. 2004. Evolution of C isotopes in the  
43 576 Cambrian of China: implications for Cambrian subdivision and trilobite mass  
44 577 extinctions. *Geobios*, **37(2)**, 287-301.
- 45  
46  
47  
48 578 ZHU, M. Y., BABCOCK, L. E., & PENG, S. C. 2006. Advances in Cambrian stratigraphy  
49 579 and paleontology: integrating correlation techniques, paleobiology, taphonomy  
50 580 and paleoenvironmental reconstruction. *Palaeoworld*, **15(3)**, 217-222.
- 51  
52  
53 581 ZHURAVLEV, A. Y., & WOOD, R. A. 1996. Anoxia as the cause of the mid-Early  
54 582 Cambrian (Botomian) extinction event. *Geology*, **24(4)**, 311-314.
- 55  
56  
57 583

584

585 Table 1. Geochemical data from both Loch Eriboll and Ardvreck Castle locations.

586 Height is measured from the base of logged sections (Fig. 2).

		<u>LOCH ERIBOLL</u>									
Original ID	Lithology	Height (m)	$\delta^{13}\text{C}_{\text{carb}}$ mean ‰ (V-PDB)	$\delta^{18}\text{O}_{\text{carb}}$ mean ‰ (VPDB)	$\delta^{13}\text{C}_{\text{org}}$ ‰ (VPDB)	wt% S	wt% Total C	TOC wt%	TIC wt%		
AS36	Sstone	0.1			-25.16	0.096	0.088	0.08	0.006		
AS37	Sstone	0.5			-25.29	0.166	0.083	0.09	-0.010		
AS38	Sstone	1			-23.84	0.229	0.844	0.03	0.815		
AS39	Sstone	1.75			-25.70	0.063	0.059	0.01	0.051		
AS40	Sstone	3.7			-25.64	0.060	0.051	0.01	0.045		
AS41	Sstone	3.8			-25.79	0.054	0.114	0.08	0.031		
AS42	Sstone	4.5			-26.40	0.324	0.030	0.02	0.015		
AS43	Sstone	5.75			-25.95	0.040	0.036	0.01	0.026		
AS44	Sstone	7.5			-24.61	0.138	1.841	0.02	1.824		
AS45	Sstone	8.25			-24.46	0.354	6.644	0.10	6.539		
AS46	Sstone	8.8	-2.98	-10.93	-22.89	0.515	4.829	0.09	4.734		
AS47	Sstone	9.15			-23.81	0.377	4.353	0.23	4.119		
AS48	Carbonate	9.75	-2.84	-11.43	-23.75	0.734	3.985	0.20	3.786		
AS49	Carbonate	10.1			-24.76	0.066	9.741	0.45	9.296		
AS50	Carbonate	10.75	-1.85	-8.52	-24.73	-0.002	8.819	0.11	8.709		
AS51	Carbonate	10.95			-25.04	-0.001	10.393	0.12	10.270		
AS52	Carbonate	11.05	-1.77	-8.99	-24.50	-0.001	8.182	0.31	7.877		
AS53	Carbonate	11.4	-1.65	-8.84	-25.64	-0.001	11.057	0.55	10.508		
AS54	Carbonate	11.8	-1.37	-8.65	-22.61	-0.001	12.71	0.68	12.031		
AS55	Carbonate	12.25			-23.36	-0.002	13.128				
AS56	Carbonate	13	-1.17	-7.83	-24.91	-0.001	13.009				
AS57	Carbonate	13.5			-24.71	0.000	12.876	0.23	12.648		
AS58	Carbonate	14.55	-0.86	-6.82	-23.23	0.027	13.166	0.88	12.290		
AS59	Carbonate	15.6	-0.97	-6.77	-21.34	0.000	12.513	0.18	12.330		
AS60	Carbonate	17.1	-1.06	-6.65	-24.34	-0.002	13.592	0.67	12.923		
AS61	Carbonate	18			-24.80	-0.001	13.326	0.72	12.606		
AS62	Carbonate	18.5	-0.38	-7.01	-23.47	-0.001	12.93	0.44	12.490		
AS63	Carbonate	20			-25.65	0.026	13.557	0.84	12.717		
AS64	Carbonate	20.55	-1.45	-6.36	-27.86	-0.002	14.057	0.91	13.149		
AS65	Carbonate	22.25	-1.36	-6.20	-25.84	0.006	13.516	1.61	11.908		
AS66	Carbonate	22.25	-1.11	-6.54	-26.87	0.003	14.281	2.58	11.705		
AS67	Carbonate	26.5	-0.81	-7.12	-24.53	0.002	13.68	4.17	9.514		
AS32	Carbonate	28.55	-0.96	-7.55		0.004	14.043	0.00	14.041		
AS33	Carbonate	28.55	-1.48	-6.67		0.014	13.937	5.16	8.780		
AS34	Carbonate	31.35	-1.60	-5.82		-0.003	13.889	4.08	9.812		
AS35	Carbonate	31.35	-1.41	-6.28	-23.07	0.019	13.171	0.58	12.588		
AS1	Carbonate	33.9	-1.49	-5.91	-27.05	-0.001	13.863	1.58	12.280		
AS2	Carbonate	34.5	-1.36	-6.50		0.007	13.92	0.00	13.918		
AS3	Carbonate	34.9	-1.60	-5.81	-25.67	-0.008	14.043	0.81	13.236		
AS4	Carbonate	35.5	-1.60	-5.28	-24.63	0.004	13.342	0.96	12.378		
AS5	Carbonate	36.1	-1.87	-5.86	-23.37	0.010	13.473	1.37	12.108		
AS6	Carbonate	36.1	-1.66	-5.90		-0.001	13.513	0.00	13.512		
AS7	Carbonate	36.75	-1.27	-5.70	-26.17	0.011	12.828	1.53	11.299		
AS8	Carbonate	37.05			-25.67	0.012	12.13	0.95	11.180		
AS9.1	Carbonate	37.2	-1.48	-5.71	-26.72	-0.002	12.906	2.39	10.521		
AS11	Carbonate	37.4			-25.98	-0.001	13.093	1.42	11.673		
AS12	Carbonate	37.8	-1.77	-6.76	-25.75	-0.009	12.49	1.05	11.442		
AS13	Carbonate	38.5			-22.82	0.005	13.284	1.35	11.931		
AS14	Carbonate	38.85	-1.61	-6.17	-23.87	0.010	13.644	1.18	12.469		
AS15	Carbonate	39.1	-1.78	-7.22	-22.20	-0.001	13.405	2.08	11.321		

AS16	Carbonate	39.55			-21.92	-0.006	13.869	1.60	12.274
AS17	Carbonate	40	-1.63	-6.40	-20.15	-0.002	13.859	2.17	11.693
AS18	Carbonate	40.95				-0.001	13.875		
AS19	Carbonate	41.75	-1.57	-6.60	-20.72	-0.002	13.767	5.19	8.577
AS20	Carbonate	42.2			-24.31	0.000	13.85	0.62	13.226
AS21	Carbonate	42.6	-1.22	-6.17	-25.47	0.000	13.679	0.72	12.959
AS22	Carbonate	43.5			-25.63	0.005	13.802	0.11	13.693
AS23	Carbonate	44	-0.91	-6.60	-25.00	0.002	13.925	0.12	13.804
AS24	Carbonate	45.5	-0.62	-6.39	-25.57	-0.002	13.599	0.29	13.311
AS25	Carbonate	47			-22.53	0.003	13.774	1.15	12.621
AS26	Carbonate	48	-0.78	-6.63	-20.93	-0.001	13.972	0.23	13.742
AS27	Carbonate	49.2			-22.21	0.004	13.974	0.51	13.462
AS29	Carbonate	51.2	-1.63	-6.63		-0.002	13.544	3.91	9.634
AS30	Carbonate	52.2			-24.97	-0.003	13.385	0.83	12.554

**ARDVRECK CASTLE**

	Original ID	Lithology	Height (m)	$\delta^{13}\text{C}_{\text{carb}}$ mean ‰ (V-PDB)	$\delta^{18}\text{O}_{\text{carb}}$ mean ‰ (VPDB)	$\delta^{13}\text{C}_{\text{org}}$ ‰ (VPDB)	wt% S	wt% C	TOC wt%	TIC wt%
SALTERELLA GRIT	VR1	Sstone	0.5	-2.09	-8.55	-27.16	0.122	1.430	0.04	1.389
	VR2	Sstone	1			-25.97	0.042	0.098	0.01	0.085
	VR3	Sstone	2			-26.26	0.071	0.050	0.01	0.038
	VR4	Sstone	3.25	-1.97	-10.73	-26.23	0.067	0.925	0.02	0.906
	VR5	Sstone	3.5	-1.51	-8.24	-26.39	0.019	6.744	0.06	6.683
	VR6	Sstone	3.75	-1.48	-7.36	-26.79	0.054	8.340	0.06	8.277
	VR7	Sstone	4	-1.20	-6.77	-27.03	-0.001	7.516	0.28	7.239
GHRUDAIDH FORMATION	VR8	Carbonate	4.2	-1.07	-6.02		0.018	12.789		
	VR9	Carbonate	4.4	-1.03	-6.08	-27.51	0.013	12.92	0.44	12.479
	VR10	Carbonate	4.6	-0.86	-5.92	-27.21	0.011	12.802	0.39	12.415
	VR11	Carbonate	4.8	-1.08	-6.28	-26.68	-0.003	8.085	0.08	8.008
	VR12	Carbonate	4.95	-0.92	-5.87	-26.78	-0.001	12.514	0.26	12.256
	VR13	Carbonate	5.1	-0.93	-5.80	-26.82	0.021	12.626	0.25	12.376
	VR14	Carbonate	5.45	-0.90	-5.62	-27.44	-0.002	12.333	0.32	12.016
	VR15	Carbonate	5.65	-0.90	-5.58	-26.84	-0.001	13.01	0.37	12.642
	VR16	Carbonate	5.95	-0.81	-5.93	-27.34	0.022	12.299	0.30	12.003
	VR17	Carbonate	6.5	-0.36	-5.80	-27.28	-0.002	12.781	0.65	12.134
	VR18	Carbonate	8.25	-0.59	-5.93	-26.20	-0.001	12.894	0.99	11.907
	VR19	Carbonate	9.5	-0.80	-6.01	-26.87	-0.001	12.663	0.47	12.193
	VR20	Carbonate	10	-1.12	-5.76	-27.62	-0.001	12.933	0.41	12.522

587

588

1  
2  
3  
4  
5  
6  
7  
8  
9  
10  
11  
12  
13  
14  
15  
16  
17  
18  
19  
20  
21  
22  
23  
24  
25  
26  
27  
28  
29  
30  
31  
32  
33  
34  
35  
36  
37  
38  
39  
40  
41  
42  
43  
44  
45  
46  
47  
48  
49  
50  
51  
52  
53  
54  
55  
56  
57  
58  
59  
60

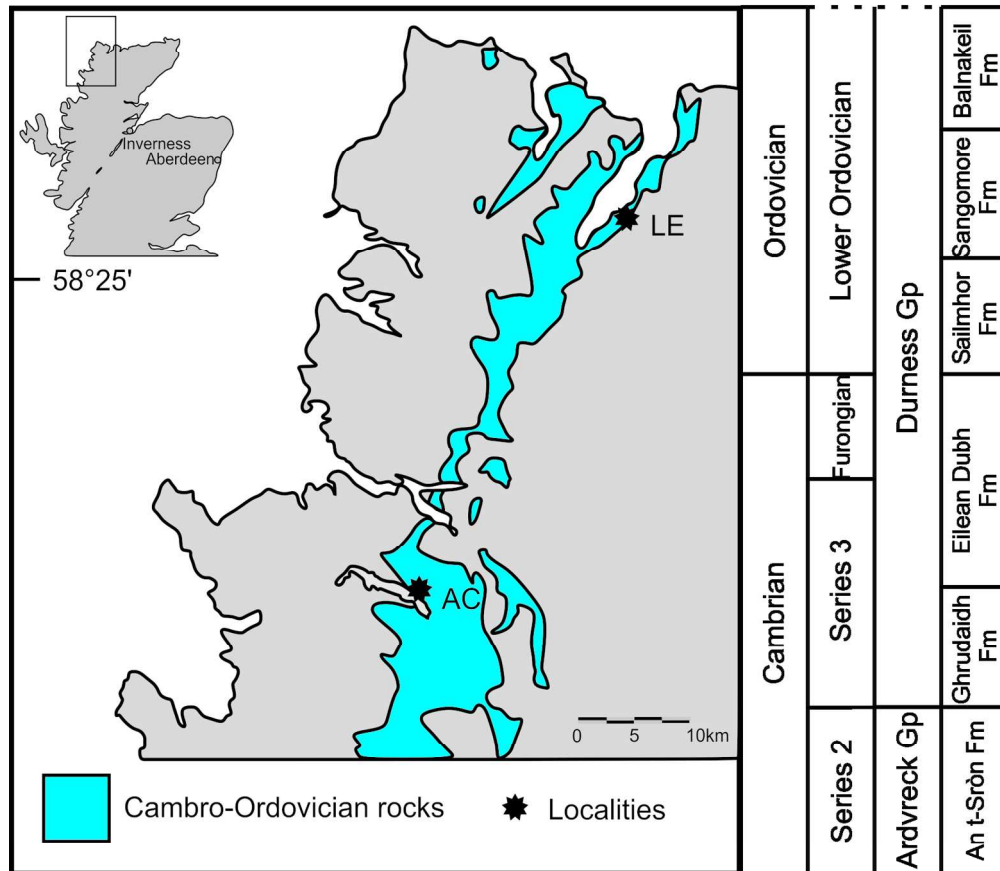


Figure 1. Locality map of the study locations (LE- Loch Eriboll, AC- Ardvreck Castle) in northwest Scotland, modified from Raine and Smith (2012), and summary of Lower-Middle Cambrian stratigraphic units in the region.

149x148mm (300 x 300 DPI)

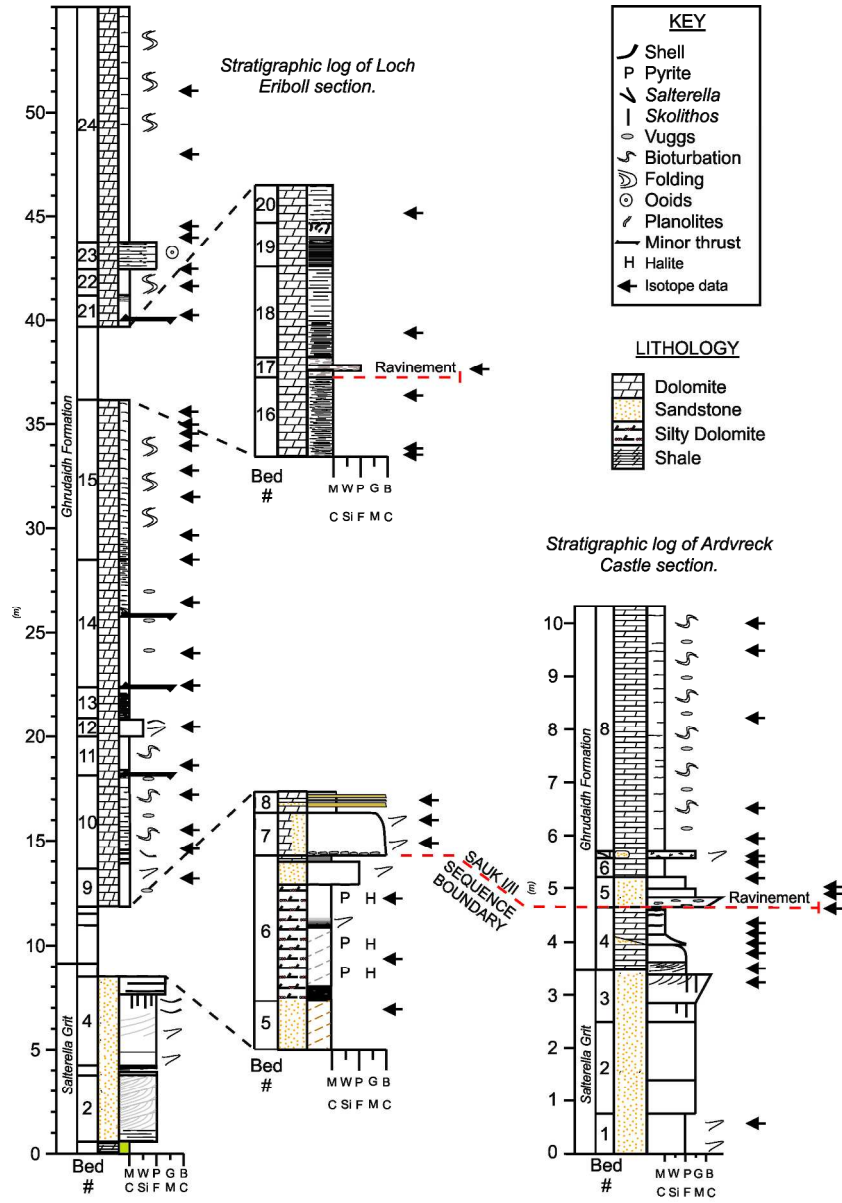


Figure 2. Sedimentary logs of the Loch Eriboll and Ardvreck Castle sections showing the correlation of a ravinement surface near the base of the Ghrudaith Formation, and a second surface ~27m above the base of the Formation at Loch Eriboll.

194x281mm (300 x 300 DPI)

1  
2  
3  
4  
5  
6  
7  
8  
9  
10  
11  
12  
13  
14  
15  
16  
17  
18  
19  
20  
21  
22  
23  
24  
25  
26  
27  
28  
29  
30  
31  
32  
33  
34  
35  
36  
37  
38  
39  
40  
41  
42  
43  
44  
45  
46  
47  
48  
49  
50  
51  
52  
53  
54  
55  
56  
57  
58  
59  
60

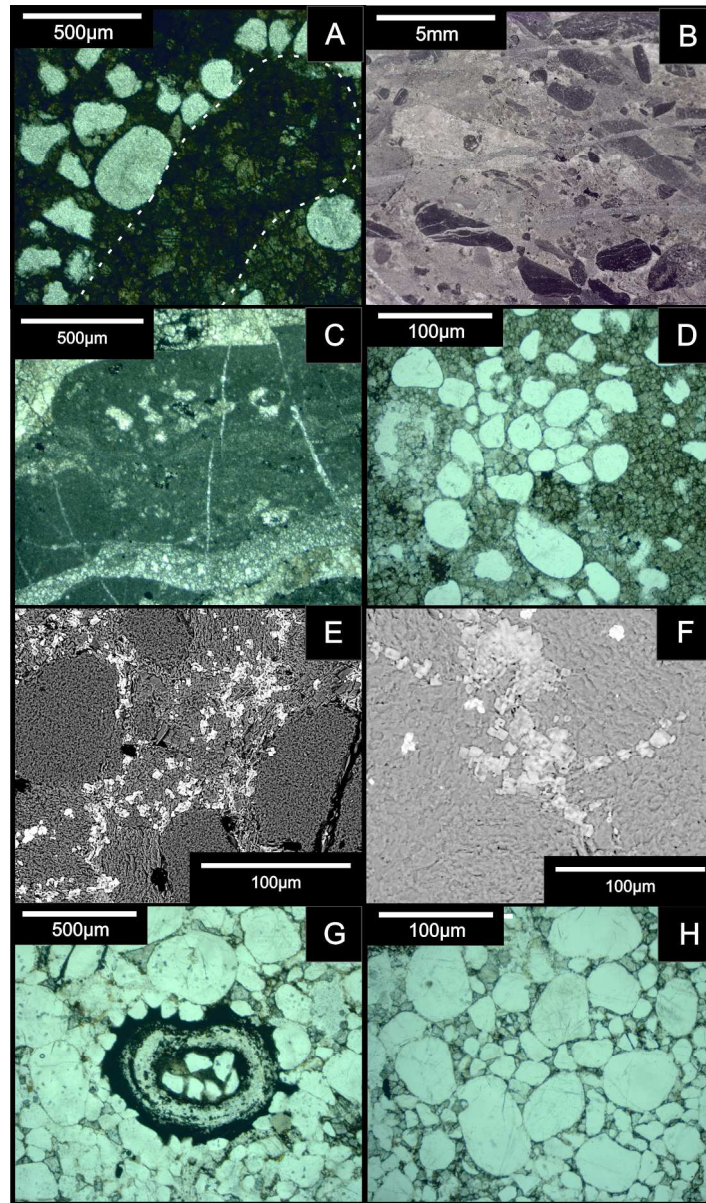


Figure 3. Photomicrographs of Ghrudaidh Formation facies. A: dolosparite pebble (highlighted with dotted line) in a sandy dolomicrite matrix, LE 17. B: Scan of slide of rudaceous limestone, exhibiting well-rounded, micrite clasts in a dolosparite matrix. C: Rudaceous limestone of bed LE17 showing irregularly shaped, sparry bioclasts in an intraclast. D: Photomicrograph of sandy/silty dolomite from the base of the Ghrudaidh Formation at Ardvreck Castle consisting of equal portions of rounded (aeolian) quartz grains and dolomite microspar (AC 3). E, F: Backscatter SEM images of LE 6 lagoonal facies. Bright white cubes are halite, mid grey is a fine dolomite matrix and the largest, dull grey grains in E are aeolian quartz silt and fine sand. G: Photomicrographs from Ardvreck Section. Salterella shell amongst well rounded quartz grains of the Salterella Grit, (Bed AC 1). H: Rounded silt and fine sand grains, a relatively poorly sorted lithology from Bed AC 1.

152x258mm (300 x 300 DPI)

1  
2  
3  
4  
5  
6  
7  
8  
9  
10  
11  
12  
13  
14  
15  
16  
17  
18  
19  
20  
21  
22  
23  
24  
25  
26  
27  
28  
29  
30  
31  
32  
33  
34  
35  
36  
37  
38  
39  
40  
41  
42  
43  
44  
45  
46  
47  
48  
49  
50  
51  
52  
53  
54  
55  
56  
57  
58  
59  
60

Proof For Review

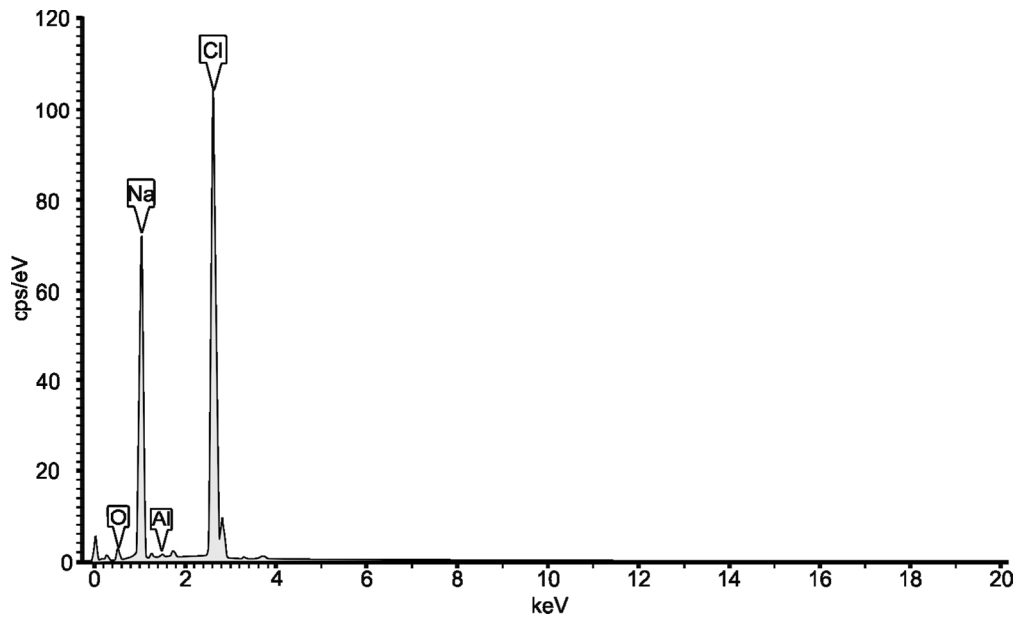


Figure 4. Representative EDS spectra taken from a halite cube in bed LE 6.

132x79mm (300 x 300 DPI)

Proof For Review

1  
2  
3  
4  
5  
6  
7  
8  
9  
10  
11  
12  
13  
14  
15  
16  
17  
18  
19  
20  
21  
22  
23  
24  
25  
26  
27  
28  
29  
30  
31  
32  
33  
34  
35  
36  
37  
38  
39  
40  
41  
42  
43  
44  
45  
46  
47  
48  
49  
50  
51  
52  
53  
54  
55  
56  
57  
58  
59  
60

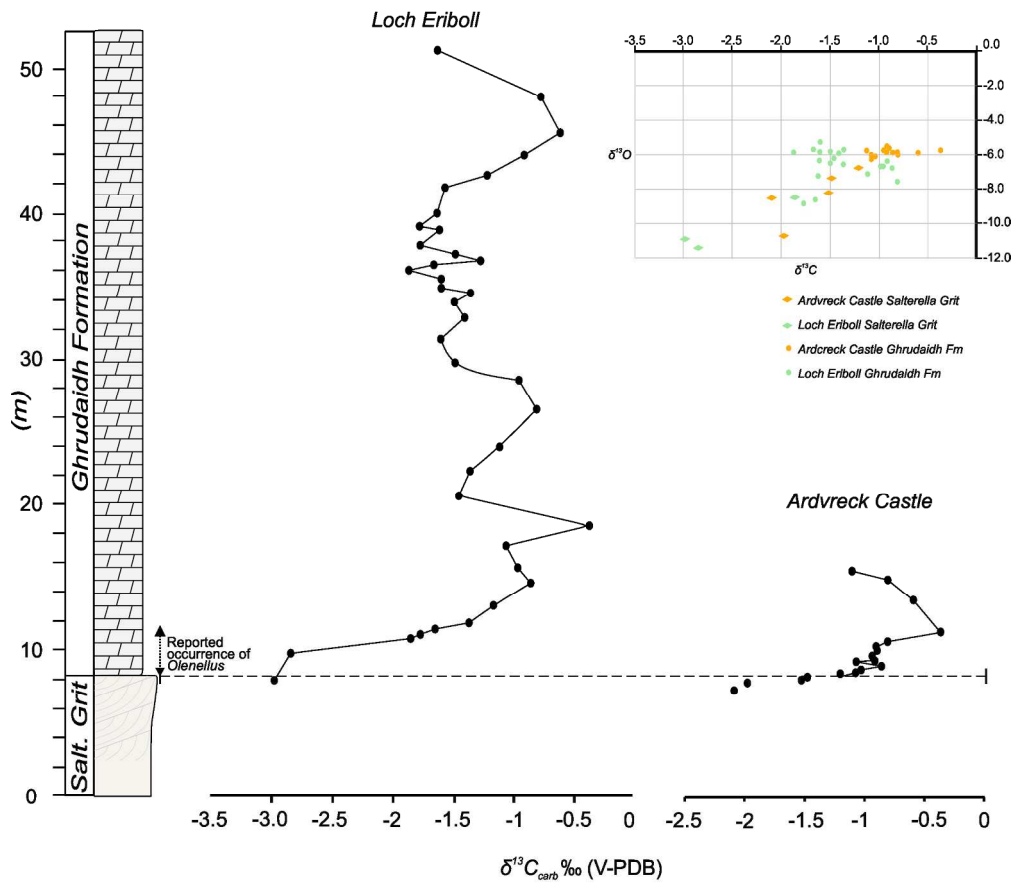


Figure 5.  $\delta^{13}C_{carb}$  chemostratigraphic curve from Loch Eriboll and Ardvreck sections. Top right inset is a cross-plot of C and O data with samples from the Salterella Grit Member and Ghrudaidh Fm from each location delineated by respective symbols. The reported occurrence of Olenellus is from Huselbee & Thomas, 1998, the precise location of the specimen is unknown but is indicated by dashed line.

205x184mm (300 x 300 DPI)



1  
2  
3  
4  
5  
6  
7  
8  
9  
10  
11  
12  
13  
14  
15  
16  
17  
18  
19  
20  
21  
22  
23  
24  
25  
26  
27  
28  
29  
30  
31  
32  
33  
34  
35  
36  
37  
38  
39  
40  
41  
42  
43  
44  
45  
46  
47  
48  
49  
50  
51  
52  
53  
54  
55  
56  
57  
58  
59  
60

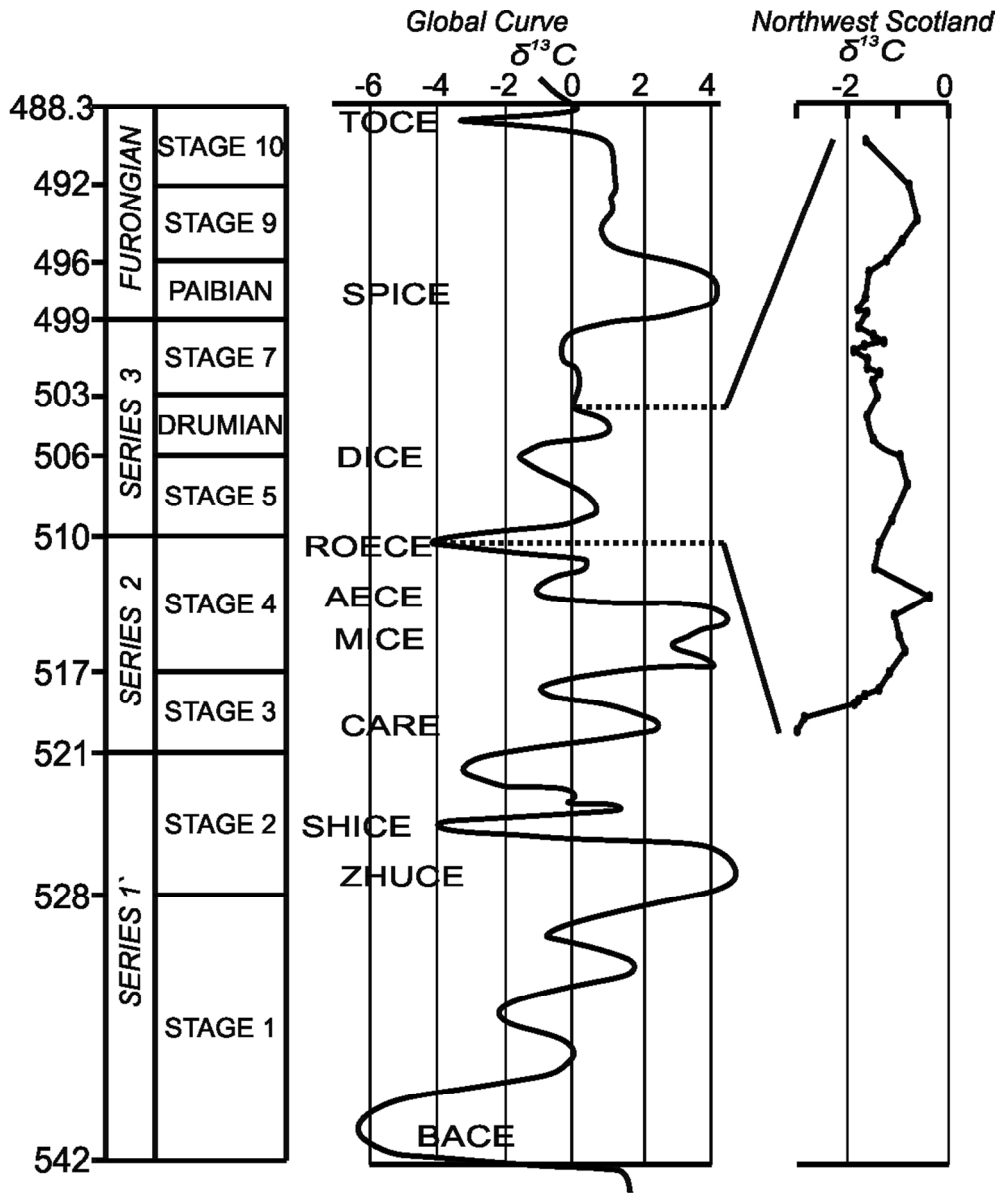


Figure 6. Global Cambrian carbon isotope curve (Zhu et al. 2006) showing the proposed correlation with the Scottish sections.

104x123mm (300 x 300 DPI)